EUSIPCO 2013 1569743351

SOFT MORPHOLOGICAL IMAGE PRIOR

Makoto NAKASHIZUKA

Faculty of Engineering, Chiba Institute of Technology
2-17-1, Tsudanuma, Narashino, Chiba, 275-0016, Japan
e-mail: nkszk@sky.it-chiba.ac.jp

ABSTRACT

This paper presents an image prior based on soft morphological filters and its application to image recovery. In morphological image processing, a gray-scale image is represented as a subset in the three dimensional space, which is spanned by spatial and intensity axes. The image is approximated as an union of the structuring elements in this space. In this paper, this morphological image model is introduced to an image prior for image recovery problem. With the proposed image prior, the image is recovered as an image that has no noise component that is eliminated by the opening and closing, which are basic operations of the morphological image processing. In our study, the closing and opening are respectively approximated as soft closing and soft opening with relaxed max and min functions in order to improve the noise robustness. Several properties of the proposed prior with the soft morphology are shown. In recovery experiments, image denoising and deblurring with the proposed prior are demonstrated. The comparison of the proposed prior with the prior based on the intensity differences are also shown.

Index Terms— Mathematical morphology, regularization, image recovery, image prior, denoising

1. INTRODUCTION

Image recovery is a problem that estimates the original image from the degraded observation. In the image recovery, an observed image $\mathbf{y}$ is supposed to be obtained via $\mathbf{y} = \mathbf{H}\mathbf{g} + \mathbf{e}$, where $\mathbf{H}$ is a degradation matrix, $\mathbf{g}$ and $\mathbf{e}$ are the original image vector and additive noise, respectively. Assuming that the noise $\mathbf{e}$ is a Gaussian noise, the estimation of the original image is obtained from the regularization[1] as

$$\hat{\mathbf{g}} \in \arg\min_{\mathbf{g}} \frac{1}{2} \parallel \mathbf{y} - \mathbf{H}\mathbf{g} \parallel_2^2 + \lambda P(\mathbf{g}). \tag{1}$$

For the image prior term $P(\mathbf{g})$, total variation (TV)[2][3] and its variants have been widely applied to image recovery. In these regularization, the local smoothness of images is assumed and is measured by the sum of the absolute gradients of intensity surface of the image. In the recovery with a sparsity prior[4], the recovered image is replaced with a linear combination of atoms in a dictionary $\mathbf{A}$ as $\mathbf{g} = \mathbf{A}\mathbf{c}$. For recovery, the sparsity prior is imposed on the coefficient vector $\mathbf{c}$. In this image prior, the linear synthesis image model is employed for image representation. On the other hand, nonlinear image models are utilized in the area of mathematical morphology[5][6][7].

In morphological image processing, a gray-scale image is transformed into an umbra of the three-dimensional space that is spanned by spatial and intensity axes. The gray-scale morphological operations are interpreted as set operations between a subset of the image and a set of *structuring elements* (SE). During the morphological image processing, an image is assumed to be a union of the set of SEs that are translated in the three dimensional space. In image opening, which is one of the morphological filters, an image is approximated by a subset of the umbra, which is a union of the set of the translated SEs. In the opening, the peaks and ridges of the intensity surface, which cannot include the translated SEs, are eliminates. On contrary, in image closing, the complement of the image is approximated by a union of the SEs. The valleys and pits, which cannot include the complements of the SEs, are eliminated by closing. Therefore, the pair of the opening and closing is used for image denoising, typically impulsive noises[7]. In denosing by the morphological filters, the original image and its complement are assumed to be a union of the translated SEs.

In this paper, a novel image prior based on the assumption of the morphological filtering is proposed. Our image prior is defined from the assumption of the opening and closing invariance. The image is recovered with the assumption that the original image has no pits and peaks that can include the SEs. In our approach, the soft-morphology filters that are approximations of the morphological filter are employed for the image prior in order to improve noise sensitivity. By using the soft morphological operations, the local smoothness can also be imposed on the recovered image.

In the next section, we briefly explain the morphological filters. The soft-morphological filters are introduced by replacing the max and min function with log-sum-exp functions[8]. Some properties of the soft morphology is also shown. In Sect. 3, the image prior using the soft morphology is presented. In Sect. 4, the proposed morphological prior is compared with the total subset variation (TSV) prior[3] that is one of the extension of TV prior in recovery experiments.

2. SOFT MORPHOLOGICAL FILTERS WITH LOG-SUM-EXP FUNCTIONS

The morphological filters are constructed from two operators, dilation and erosion[5][6][7]. Let $\mathcal{I}$ be a set of two-dimensional coordinates of the image. Each element in $\mathcal{I}$ is a two-dimensional vector, whose two coordinates are integers. $f_{\mathbf{x}}$ denotes the intensity of an image f at the coordinate $\mathbf{x} \in \mathcal{I}$. The dilation and erosion of the gray-scale image f are respectively defined as

$$D_s \circ f_{\mathbf{x}} = \bigvee_{\mathbf{y} \in \mathcal{A}} f_{\mathbf{x}+\mathbf{y}} + s_{\mathbf{y}} \tag{2}$$

and

$$E_s \circ f_{\mathbf{x}} = \bigwedge_{\mathbf{y} \in \mathcal{A}} f_{\mathbf{x}-\mathbf{y}} - s_{\mathbf{y}}, \tag{3}$$

where $\bigvee_{\mathbf{y} \in \mathcal{A}}$ and $\bigwedge_{\mathbf{y} \in \mathcal{A}}$ denote the maximum and minimum value of the elements with respect to the set of $\mathcal{A}$, respectively. $\{s_{\mathbf{x}}\}_{\mathbf{x} \in \mathcal{A}}$ is the SE for the morphological filtering. The morphological opening obtains an approximation of the image in the form of the dilation in (2). For image opening, the dilation is applied to the eroded image of f as follows:

$$O_s \circ f_{\mathbf{x}} = D_s \circ E_s \circ f_{\mathbf{x}}. \tag{4}$$

Obviously, the dilated images are invariant with respect to the opening. The opened image always satisfies

$$f_{\mathbf{x}} \geq O_s \circ f_{\mathbf{x}}. \tag{5}$$

This property is referred to as the antiextensivity of the opening. The closing, which is the complementary operation of the opening, is realized as

$$C_s \circ f_{\mathbf{x}} = E_s \circ D_s \circ f_{\mathbf{x}}. \tag{6}$$

The complement of the closed image includes the original image. Therefore, the closed image always satisfies

$$f_{\mathbf{x}} \leq C_s \circ f_{\mathbf{x}}. \tag{7}$$

The eroded images are invariant with respect to the closing. The opening can eliminate only positive noise components, which cannot include SEs. In contrast, the closing can eliminate only negative noise components. The results of the opening and closing are hence sensitive for the noise which has both of the negative and positive components. In order to reduce the noise sensitivity of the morphological processing, the soft morphology operators[9][10] have been proposed. In these approach, the max and min functions are relaxed by weighted statistic[10], soft max and min functions[11]. In this study, the soft morphological filters are simply constructed by replacing the max and min functions with log-sum-exp functions[8]. By using the log-sum-exp function, we have approximations of the dilation (2) and erosion (3) as

$$\hat{D}_s \circ g_{\mathbf{x}} = \frac{1}{p} \log \sum_{\mathbf{y} \in \mathbb{A}} \exp\left(p\left(g_{\mathbf{x}+\mathbf{y}} + s_{\mathbf{y}}\right)\right) \tag{8}$$

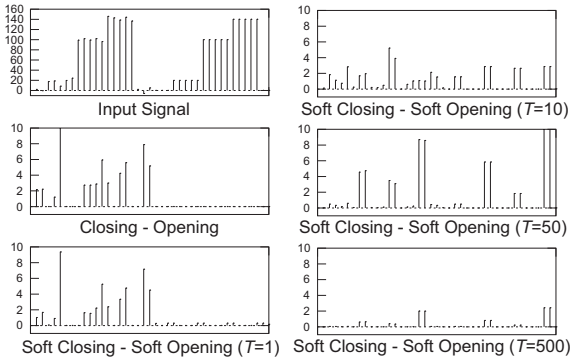

Fig. 1. Differences between closing and opening at various approximation parameters.

and

$$\hat{E}_s \circ g_{\mathbf{x}} = -\frac{1}{p} \log \sum_{\mathbf{y} \in \mathbb{A}} \exp\left(-p\left(g_{\mathbf{x}-\mathbf{y}} - s_{\mathbf{y}}\right)\right), \tag{9}$$

where $p > 0$ is the parameter that specifies the bounds of the approximation error,

$$0 \leq \hat{D}_s \circ f_{\mathbf{x}} - D_s \circ f_{\mathbf{x}} \leq \frac{1}{p} \log N \tag{10}$$

and

$$-\frac{1}{p} \log N \leq \hat{E}_s \circ f_{\mathbf{x}} - E_s \circ f_{\mathbf{x}} \leq 0 \tag{11}$$

where N is the number of the elements in $\mathcal{A}$. When $p \to \infty$, the approximations converge to true erosion and true dilation. The soft opening and soft closing can also be constructed as $\hat{O}_s \circ f_{\mathbf{x}}$ and $\hat{O}_s \circ f_{\mathbf{x}}$ by replacing the erosion and dilation with the soft erosion and soft dilation. For $p \to \infty$, the soft opening and soft closing converge to true opening and true closing, respectively. For $p \to 0$, the soft opening and soft closing converge to

$$\begin{aligned} \lim_{p \to 0} \hat{O} \circ f_{\mathbf{x}} &= \lim_{p \to 0} \hat{C} \circ f_{\mathbf{x}} \\ &= \frac{1}{N^2} \sum_{\mathbf{y} \in \mathcal{A}} \sum_{\mathbf{z} \in \mathcal{A}} f_{\mathbf{x}+\mathbf{y}-\mathbf{z}} - s_{\mathbf{z}} + s_{\mathbf{y}} \end{aligned} \tag{12}$$

along with the L'Hôpotal's rule. The soft opening and soft closing, of which max and min are approximated with log-sum-exp functions, are continuously differentiable functions. The gradient based minimization can be applied to the function that includes the soft opening and soft closing. We apply these soft morphological filters for image recovery problem in (1).

3. IMAGE PRIOR USING SOFT-MORPHOLOGICAL FILTERS

In this section, we propose the image prior for the recovery problem (1) with morphological filter invariance. We assume

that the image $\mathbf{g}$ can be represented as a union of the translated SEs in the form of (2). If this assumption is held , the image $\mathbf{g}$ is invariant with the opening. Under this assumption, the prior term is defined as the absolute difference between the image and its opened version as

$$P_O(\mathbf{g}) = \sum_{\mathbf{x}\in\mathcal{I}} |g_{\mathbf{x}} - O_s \circ g_{\mathbf{x}}| = \sum_{\mathbf{x}\in\mathcal{I}} g_{\mathbf{x}} - O_s \circ g_{\mathbf{x}}. \quad (13)$$

By substituting the soft opening (13) and supposing every elements of the SE are zero, the opening invariance prior can be approximated as

$$\hat{P}_O(\mathbf{g}) = -\frac{1}{p}\sum_{\mathbf{x}\in\mathcal{I}} \log \sum_{\mathbf{y}\in\mathcal{A}} \frac{1}{1+\sum_{\mathbf{z}\in\mathcal{A},\mathbf{z}\neq\mathbf{y}} \exp\{p\,(f_{\mathbf{x}-\mathbf{y}+\mathbf{z}} - f_{\mathbf{x}})\}}. \quad (14)$$

This function monotonically increases along with the increment of the intensity difference $f_{\mathbf{x}-\mathbf{y}+\mathbf{z}} - f_{\mathbf{x}}$. Closing invariance can be also imposed on the image recovery. The closing invariance prior is defined as

$$P_C(\mathbf{g}) = \sum_{\mathbf{x}\in\mathcal{I}} |g_{\mathbf{x}} - C_s \circ g_{\mathbf{x}}| = \sum_{\mathbf{x}\in\mathcal{I}} C_s \circ g_{\mathbf{x}} - g_{\mathbf{x}}. \quad (15)$$

With this prior, the image is recovered under the assumption that the complementary of the image is a union of the translated SEs. The approximation of P_C is given by the soft closing as

$$\hat{P}_C(\mathbf{g}) = -\frac{1}{p}\sum_{\mathbf{x}\in\mathcal{I}} \log \sum_{\mathbf{y}\in\mathcal{A}} \frac{1}{1+\sum_{\mathbf{z}\in\mathcal{A},\mathbf{z}\neq\mathbf{y}} \exp\{p\,(f_{\mathbf{x}} - f_{\mathbf{x}+\mathbf{y}-\mathbf{z}})\}} \quad (16)$$

where the elements of the SE are supposed to be zero. The soft closing prior monotonically increases along with the increment of the intensity difference $f_{\mathbf{x}} - f_{\mathbf{x}+\mathbf{y}-\mathbf{z}}$. In this study, an image prior is proposed by adding two prior according to the closing and opening invariance as

$$\hat{P}_{OC}(\mathbf{g}) = \hat{P}_O(\mathbf{g}) + \hat{P}_C(\mathbf{g}) = \sum_{\mathbf{x}\in\mathcal{I}} \hat{C}_s \circ g_{\mathbf{x}} - \hat{O}_s \circ g_{\mathbf{x}}. \quad (17)$$

Hereinafter, we refer to this prior as the close-open invariance prior. For $p \to \infty$, this prior is defined as the sum of the differences between the closing and the opening of the image. In this case of the image recovery (1) with the close-open invariance, the image is assumed to be an image that has no noise component that is eliminated by the opening and closing. For bounded p, this prior increases along with the intensity differences between the pixel and each surrounding pixel as seen in (15) and (17). For $p \to 0$, both filters converge to a linear filter in (13) and the prior term P_{OC} converges to zero. In Fig. 1, examples of the difference between the closing and opening for a one-dimensional signal are shown. In these examples, the SE spans within two consecutive samples as $\{s_0, s_1\} = \{0, 0\}$. The input signal for the morphological filters is shown in the top of the left column of Fig. 1. The signal consists of two periods, of which first period is degraded by a random noise. The second period of the signal is invariant with respect to closing and opening with the SE. In the second row of the left column, P_{OC}, which is difference between the closing and opening is shown. The amplitude of P_{OC} increases due to the noise components in the first period. For the second period, P_{OC} is zero, since the signal holds the opening and closing invariance. In the others, $\hat{P}_{OC}$ with various approximation parameters p are shown. When $p = 1$, the differences between the approximation and P_{OC} are relatively small. At $p = 0.1$, $\hat{P}_{OC}$ responds to the intensity differences between consecutive two samples in the second period. Along with the decrement of p, the amplitude of $\hat{P}_{OC}$ tends to be proportional to the absolutes of the intensity differences. As seen in these example, the approximated close-open invariance prior can impose the penalty on the intensity variations and the structure of the signal according to the closing and opening invariance simultaneously with appropriate parameter p.

By the way, the total subset variation (TSV) prior, which is an extension of TV prior, has been proposed in Ref. [3]. The TSV is defined from the difference between the maximum and minimum of the local clique. Therefore, the TSV can be represented by the notations of the mathematical morphology as

$$P_{TSV}(\mathbf{g}) = \sum_{\mathbf{x}\in\mathcal{I}} \{D_s \circ g_{\mathbf{x}} - E_s \circ g_{\mathbf{x}}\}^q \quad (18)$$

where the all elements of the SE are zero. When $q = 1$ and the SE is defined within four neighbors, the TSV is equivalent of the standard TV[3]. In the proposed prior, the dilation and erosion of the TSV are respectively replaced with the opening and closing. In the recovery with the TSV, the prior impose the penalty on the differences of the intensities within the clique that is specified by the SE. With the close-open invariance prior, the penalty is imposed on the structure of the image according to the opening and closing invariance. The comparison the TSV with the proposed penalty is demonstrated in the next section.

4. IMAGE RECOVERY EXAMPLES

In this section, we provide several examples of the image recovery with the close-open invariance prior. For our prior, images and its complementaries are supposed to be a union of the translated SEs. Images that can be recovered with the proposed prior are limited by the image model that is employed for the morphological image processing. Under this limitation, we employ three images shown in Fig. 2 for recovery examples. The QR code shown in Fig. 2(a) is exactly opening

Fig. 2. Original images, (a) QR, (b) Cartoon and (c) Fingerprint.

Table 1. MSEs of the denoised images by the close-open invariance prior and TSV.

Image	Noise Var. σ^2	C-O Inv. $p = 1$	C-O Inv. $p = 0.1$	TSV
QR	500	99	54	99
	1000	208	78	195
	2000	429	156	387
	4000	776	394	723
Cartoon	500	227	151	155
	1000	339	236	264
	2000	518	368	443
	4000	840	528	697
Fingerprint	500	224	140	155
	1000	326	208	264
	2000	501	286	443
	4000	794	467	697

and closing invariant with the SE that can be included in each square block. Fig. 2(b) and (c) consist of lines that can be approximated as a union of the translated SEs, of which size is smaller than the width of the lines. For these images, the SE is specified as 3×3 flat square. In order to solve the problem (1), we employ limited memory BFGS (L-BFGS) [11] that is one of quasi newton methods. The objective function with the close-open invariance prior is not convex. The iteration of the minimization converges to a saddle point or local minimum. The results of the recovery depend on the initial image for the minimization. We specify the initial images as the observed images for all examples.

First, several examples of the denoising are demonstrated. For image denoising, the degradation matrix $\mathbf{H}$ is an identity matrix. The degraded images are generated by adding the Gaussian noise with the variance σ^2 to the original images. The intensities of pixels that exceed the maximum intensity level 255 are rounded to 255. For comparison, the results obtained by the TSV prior are also shown. In the regularization (1), the parameter λ has to be specified. For the purpose of the comparison, λ is specified to minimize the MSE for both the TSV and the close-open invariance prior. The TSV is defined with the clique that spans within 3×3 pixels as well as the SE that is employed for close-open prior. TSV in (19)

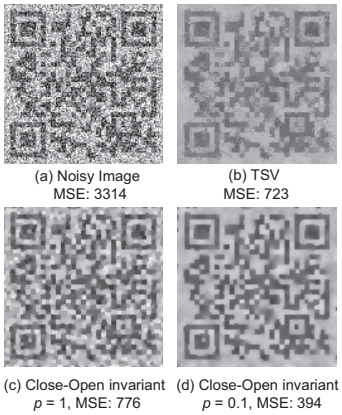

Fig. 3. Denoising results of QR. (a) Noisy image degraded by Gaussian noise $\sigma^2 = 4,000$, (b) image recovered by TSV and (c, d) close-open invariant prior.

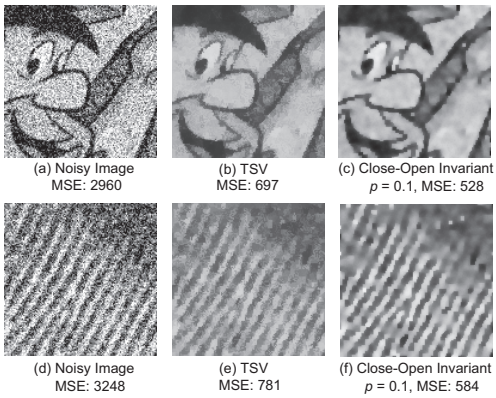

Fig. 4. Denoising results of Cartoon and Fingerprint. (a, d) Noisy images degraded by Gaussian noise $\sigma^2 = 4,000$, (b, e) images recovered by TSV and (c, f) close-open invariant prior.

has an exponential part q. Obviously, the close-open prior can be extended with the exponential part. For comparison, q is specified as $q = 1$.

MSEs (Mean Square Errors) of the denoising results are shown in Table 1. In this table, the approximation parameter p is specified as 1 and 0.1. Comparing the case of $p = 1$ with $p = 0.1$, the MSEs obtained with $p = 0.1$ are smaller than the MSEs with $p = 1$. In Fig. 3, the denoising results of QR are shown. With $p = 1$, the denoised image consists of small blocks that are correspond to the SE and hold open-close invariance. However, large artifacts due to the discontinuities due to the blocks appear. As seen in Fig. 1, the variations of the intensity are penalized with smaller p. Therefore, the block artifacts are well suppressed in the recovery result Fig. 3 (d) with $p = 0.1$. Comparing with TSV, the close-open invariant with $p = 0.1$ obtains superior results for all

Table 2. MSEs of the deblurred images by the close-open invariance prior and TSV.

Imega	Noise Var. σ^2	C-O Inv. $p = 0.1$	TSV
QR	50	251	241
	100	387	380
Cartoon	50	377	365
	100	415	405
Fingerprint	50	319	360
	100	387	383

images. In Fig. 4, the results for Cartoon and Fingerprint images are shown. Two images are not exactly close-open invariant. Therefore, the improvements of MSE comparing with the TSV are smaller than the QR image for smaller noise variances. However, the significant improvements appear at the higher noise variances.

Next, the deblurring examples are shown. In these examples, the degraded image is generated by the blurring with the Gaussian kernel with the standard deviation 2.0 and adding Gaussian noises with variances σ^2. The results in MSEs of the recovered image is shown in Table 2. An example of the recovered image is shown in Fig. 5. In deblurring, the significant differences between the TSV and close-open invariant are not observed. For deblurring, the TSV prior that suppress the intensity variations is enough to reduce the noise components during the recovery.

5. CONCLUSIONS

In this paper, the image prior based on the soft morphological filters is proposed. We show some properties of the soft opening and soft closing and applied to the image prior. With the proposed prior, the image is recovered as a close-open invariant image. Moreover, the intensity differences is penalized by the proposed prior with the the approximation parameter. In the recovery experiments, we show that the proposed prior obtains superior results for the denoising of the images that can be approximated as unions of the SEs comparing with the prior based on the intensity differences.

Usually, occurrences of the Gaussian noises are not considered in the morphological image processing. In our approach, the morphological filters are utilized for the prior of the regularization and achieve the suppression of the Gaussian noises. It is expected that the robustness of morphological image processing against Gaussian noises will be improved by using our approach. For the proposed prior, the approximation parameter p has to be specified. In this paper, we specify this parameter experimentally. Moreover, the recovery capability can be improved with the SE that is adopted to the image structure. The parameter specification and adaptation of the SE for specific application are also future topics.

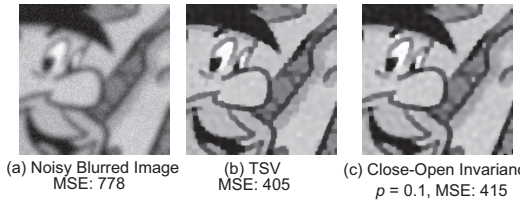

Fig. 5. Deblurring results of Cartton. (a) Degraded image ($\sigma^2 = 100$) (b) image recovered by TSV and (c) close-open invariant prior.

6. REFERENCES

[1] P. C. Hansen, J. G. Nagy and D. P. O'Leary DEBLURRING IMAGES, MATRICES, SPECTRA AND FILTERSING, SIAM, 2006.

[2] L. I. Rudin, S. Osher and E. Fatemi, "Nonlinear total variation based noise removal algorithms," Phys. D, vol. 60, no. 1-4, pp. 259-268, 1992.

[3] S. Kumar and T. Q. Nguyen, "Total subset variation prior, " Proc. of IEEE Int. Conf. on Image Processing, pp. 77-80, Hong Kong, Sept. 2010.

[4] M. Elad, SPARSE AND REDUNDANT REPRESENTATION, Springer, 2009.

[5] J. Serra, IMAGE ANALYSIS AND MATHEMATICAL MORPHOLOGY, New York, Academic, 1982.

[6] P. Maragos and R. W. Scafer, "Morphological filters - part I: their set-theoretical analysis and relations to linear shift-invariant filters, " IEEE on ASSP, vol. 35, no. 8, pp. 1153-1169, Aug. 1987.

[7] P. Maragos, Morphological filtering for image enhancement and feature detection, Chapter 3. 3 for the Book: The Image and Video Processing Handbook, A. C. Bovik Ed., Elsevier Academic Press, pp. 135-156, 2005.

[8] S. Boyd and L. Vandenberghe, CONVEX OPTIMIZATION, Cambridge University Press, 2004.

[9] A. Yuille, L. Vincent and D. Geiger, "Statistical morphology and bayesian reconstruction, " Journal of Mathematical Imaging and Vision, vol. 1, no. 3, pp. 223-238, Sept. 1992.

[10] P. Kuosmanen and J. Astola, "Soft morphological filtering, " Journal of Matehmatical Imaging and Vision, " vol. 5, no. 3, pp. 231-262, Sept. 1995.

[11] J. Nocedal and S. J. Wright, NUMERICAL OPTIMIZATION, Springer, 1999.